

Prospects for constrained supersymmetry at $\sqrt{s} = 33$ TeV and $\sqrt{s} = 100$ TeV proton–proton super-colliders

Andrew Fowlie^a, Martti Raidal^b

National Institute of Chemical Physics and Biophysics, Ravala 10, Tallinn 10143, Estonia

Received: 5 May 2014 / Accepted: 17 June 2014 / Published online: 11 July 2014
© The Author(s) 2014. This article is published with open access at Springerlink.com

Abstract Discussions are under way for a high-energy proton–proton collider. Two preliminary ideas are the $\sqrt{s} = 33$ TeV HE-LHC and the $\sqrt{s} = 100$ TeV VLHC. With Bayesian statistics, we calculate the probabilities that the LHC, HE-LHC, and VLHC discover SUSY in the future, assuming that nature is described by the CMSSM and given the experimental data from the LHC, LUX, and Planck. We find that the LHC with 300/fb at $\sqrt{s} = 14$ TeV has a 15–75 % probability of discovering SUSY. Should that run fail to discover SUSY, the probability of discovering SUSY with 3000/fb is merely 1–10 %. Were SUSY to remain undetected at the LHC, the HE-LHC would have a 35–85 % probability of discovering SUSY with 3000/fb. The VLHC, on the other hand, ought to be definitive; the probability of it discovering SUSY, assuming that the CMSSM is the correct model, is 100 %.

1 Introduction

Supersymmetry [1–3] (SUSY) is the most popular scenario of new physics beyond the Standard Model (SM). It stabilizes the electroweak scale against radiative corrections from any high-scale physics such as a Grand Unified Theory [4,5] (GUT), predicts gauge coupling unification, and provides a natural framework for explaining the observed amount of dark matter (DM) via a thermal relic density of the lightest supersymmetric particle [6]. Despite a huge experimental effort in the last few years, no clear experimental evidence for the existence of SUSY has been found so far in collider experiments, direct and indirect searches for DM or in precision physics. The Large Hadron Collider (LHC) upgrade with a center-of-mass energy of $\sqrt{s} = 14$ TeV and proposed future colliders, such as the High-Energy LHC (HE-LHC) [7] with $\sqrt{s} = 33$ TeV or the Very Large Hadron

Collider (VLHC) with $\sqrt{s} = 100$ TeV (see *e.g.*, Ref. [8]) could, therefore, play a crucial role in deciding the fate of SUSY.

Direct hadron collider searches for SUSY and indirect searches for DM are complementary; hadron collider searches are predominantly sensitive to the masses and mass hierarchies of the colored sparticles, whereas indirect searches for DM are sensitive to the mass and character (*i.e.*, gaugino and higgsino admixture) of the neutralino. We include LHC and indirect searches in our analysis.

The aim of this paper is to quantify with Bayesian statistics the probability of discovering the Constrained Minimal Supersymmetric Standard Model (CMSSM) at the $\sqrt{s} = 14$ TeV LHC, HE-LHC, and VLHC, given that previous experiments found no discrepancies with the predictions of the SM. We choose to work with the CMSSM because it is the best-known SUSY model with non-degenerate mass spectra. We believe that our results help to motivate building the HE-LHC and the VLHC, and that they contribute to forming research programs for those colliders.

Given our assumptions, we find that there is an appreciable probability that the LHC or HE-LHC could discover the CMSSM. However, the VLHC would be definitive—either the VLHC discovers the CMSSM or one has to relax some of the assumptions we have made. This conclusion results from the fact that the CMSSM mass spectrum cannot be arbitrarily heavy, else the Higgs mass would be greater than ~ 125 GeV and the DM abundance could not be explained with thermal freeze-out processes. Since those are physical requirements, a similar conclusion must be obtained for other SUSY models with similar numbers of free parameters. Our results do not apply to SUSY models with compressed mass spectra [9], which could evade searches for missing transverse momentum, or to models with extended particle content, such as the NMSSM [10,11], that have additional tree-level contributions to the Higgs boson mass as well as new candidates for DM. Those models deserve separate dedicated studies.

^a e-mail: Andrew.Fowlie@KBFL.ee

^b e-mail: Martti.Raidal@CERN.ch

The paper is organized as follows. In the next section we present the basics of Bayesian statistics on which our methodology is based. In Sect. 3, we calculate the posterior pdf and in Sect. 4, we discuss which parts of the CMSSM parameter space might be discoverable at the LHC $\sqrt{s} = 14$ TeV, a $\sqrt{s} = 100$ TeV VLHC or a $\sqrt{s} = 33$ TeV HE-LHC and complete our calculation, finding the probability that a collider could find constrained supersymmetry.

2 Bayesian approach

To quantify statements such as, “the probability that the HE-LHC could discover constrained supersymmetry,” we invoke Bayesian statistics. We remind the reader that in Bayesian statistics, probability is a numerical measure of belief in an hypothesis. See *e.g.*, Ref. [12] for a pedagogical introduction.

From an experiment, one can construct a “likelihood function,” describing the probability of obtaining the data, given a particular point, \vec{x} , in a model’s parameter space,

$$\mathcal{L}(\vec{x}) = p(\text{data} | \vec{x}, \text{model}). \tag{1}$$

The likelihood function for a measurement is typically a Gaussian function (by the central limit theorem). Note that the likelihood function, however, is not a probability distribution function (pdf). Bayes’ theorem,

$$p(a | b) = \frac{p(b | a)p(a)}{p(b)}, \tag{2}$$

permits us to “invert” the likelihood function to find the probability density of the model’s parameter space, given the data;

$$p(\vec{x} | \text{data}, \text{model}) = \frac{p(\text{data} | \vec{x}, \text{model})p(\vec{x} | \text{model})}{p(\text{data} | \text{model})}. \tag{3}$$

This quantity, which we shall call the “posterior,” is central to our work; it is a numerical measure of our belief in the parameter space *after* seeing the experimental data. On the other hand, $\pi(\vec{x}) \equiv p(\vec{x} | \text{model})$, the “prior,” is a numerical measure of our belief in the parameter space *before* seeing the experimental data. For our purposes, the denominator is merely a normalization factor. One can see that the likelihood function “updates” our prior beliefs with experimental data, resulting in our posterior beliefs.

The posterior is a pdf of the continuous model parameters \vec{x} . As such, if we wish to find the probability within a region of parameter space, we integrate (in the lexicon of Bayesian statistics, “marginalize”), *e.g.*,

$$p(\vec{x} \in A | \text{data}, \text{model}) = \int_A p(\vec{x} | \text{data}, \text{model}) \prod dx. \tag{4}$$

In our analysis, the model is the Constrained Minimal Supersymmetric Standard Model (CMSSM) [13–15], the data is that from, *inter alia*, the LHC, LUX, and Planck, and \vec{x} is a

parameter point in the CMSSM. The CMSSM has four continuous parameters, that is, three soft-breaking parameters ($m_{1/2}$, m_0 and A_0) and the ratio of the Higgs vevs ($\tan \beta$), and one discrete parameter, the sign of the Higgs parameter in the superpotential ($\text{sign } \mu$).

We assume that particular regions of our model’s parameter space would be discoverable at the *e.g.*, VLHC, whereas the complement of those regions would be entirely inaccessible;

$$p(\text{Discoverable at VLHC} | \vec{x}, \text{model}) = \begin{cases} 1 & \text{if } \vec{x} \in \text{Discoverable,} \\ 0 & \text{if } \vec{x} \notin \text{Discoverable.} \end{cases} \tag{5}$$

We find the probability that a point is discoverable by marginalizing;

$$p(\text{Discoverable} | \text{data}, \text{model}) = \int p(\text{Discoverable} | \vec{x}, \text{model})p(\vec{x} | \text{data}, \text{model}) \prod dx, \tag{6}$$

for which we rely on the fact that

$$p(\text{Discoverable} | \text{data}, \vec{x}, \text{model}) = p(\text{Discoverable} | \vec{x}, \text{model}), \tag{7}$$

i.e., whether a point in a model’s parameter space is discoverable is dependent on only the point itself, and not on any previous measurements. Combining our Eq. (5) with Eq. (6), we find our desired result,

$$p(\text{Discoverable} | \text{data}, \text{model}) = \int_{\text{Discoverable}} p(\vec{x} | \text{data}, \text{model}) \prod dx. \tag{8}$$

It can be shown that

$$p(\text{Discoverable, model} | \text{data}) \approx p(\text{Discoverable} | \text{data}, \text{model})\pi(\text{model}), \tag{9}$$

but it is an approximation that is reasonable only if no particular models are favored by the experimental data, *i.e.*, one should not, in general, multiply probabilities from Eq. (8) by his prior for the model in question; the normalization of the result will be incorrect.

3 Posterior maps of the CMSSM

We wish to calculate the posterior density of the CMSSM, given the experimental data in Table 1, which includes the Higgs mass, dark matter constraints, which we assume to be the lightest neutralino, *b*-physics observables, electroweak precision observables and the anomalous magnetic moment of the muon (see *e.g.*, Ref. [16–27] for similar analyses).

Table 1 Experimental data included in our likelihood function. Note that in the case of $\text{BR}(B_u \rightarrow \tau \nu)/\text{BR}(B_u \rightarrow \tau \nu)|_{\text{SM}}$, the error listed is a combined theory and experimental error from Ref. [55]

Quantity	Experimental data, $\mu \pm \sigma$	Theory error, τ
Ωh^2	0.1199 ± 0.0027 [43]	10 % [44,45]
m_h	125.9 ± 0.4 GeV [46–48]	2.0 GeV [49]
δa_μ	$(28.8 \pm 7.9) \times 10^{-10}$ [46]	1.0×10^{-10} [50]
M_W	80.399 ± 0.023 GeV [46]	0.015 GeV [50]
$\sin^2 \theta_{\ell, \text{eff}}$	0.23116 ± 0.00013 GeV [46]	0.00015 GeV [50]
ΔM_{B_s}	17.77 ± 0.12 GeV [46]	2.4 GeV [51]
$\text{BR}(B_s \rightarrow \mu\mu)$	$(3.2 \pm 1.5) \times 10^{-9}$ [46]	14 % [52]
$\text{BR}(B_s \rightarrow X_s \gamma)$	$(3.43 \pm 0.22) \times 10^{-4}$ [53]	0.21×10^{-4} [54]
$\text{BR}(B_u \rightarrow \tau \nu)/\text{BR}(B_u \rightarrow \tau \nu) _{\text{SM}}$	1.43 ± 0.43 [55]	
ATLAS 20.1/fb at $\sqrt{s} = 8$ TeV [38]		
LUX 85.3 live-days [41] with a factor of 10 uncertainty in σ_p^{SI} [42]		

The two ingredients that we require are the likelihood function and the priors in Eq. (3). We will supply these ingredients to the nested sampling algorithm implemented in MultiNest-2.18 [28] via PyMultiNest [29], which will return the posterior. See e.g., Ref. [30] for a detailed introduction to the methodology. micrOMEGAS-2.4.5 [31,32] and FeynHiggs-2.9.4 [33–36]. We construct Gaussian likelihoods for these experiments, including theory errors in quadrature. Our likelihood function is thus the product of these Gaussian functions,

$$\mathcal{L}(\vec{x}) = \prod \exp \left[-\frac{(p_i(\vec{x}) - \mu_i)^2}{2(\sigma_i^2 + \tau_i^2)} \right], \tag{10}$$

where $p(\vec{x})$ is our model’s prediction at parameter point \vec{x} , μ , σ , and τ are the mean, experimental error and theory error, respectively, and the product is taken over the data in Table 1. We calculate the CMSSM’s predictions with SOFTSUSY-3.3.7 [37], micrOMEGAS-2.4.5 [31,32] and FeynHiggs-2.9.4 [33–36]. Furthermore, we veto CMSSM points excluded at 95 % by LHC direct searches. We apply the 95 % exclusion contour from the ATLAS search in 20.1/fb at $\sqrt{s} = 8$ TeV [38] as a hard-cut on the $(m_0, m_{1/2})$ plane. Although Ref. [38] assumed that $\tan \beta = 30$, $A_0 = -2m_0$, and $\mu > 0$, Ref. [22,39,40] demonstrated that the 95 % exclusion contour on the $(m_0, m_{1/2})$ plane is independent of $\tan \beta$, A_0 and $\text{sign } \mu$. We implement the LUX direct search for dark matter [41] with an exclusion contour on the $(m_{\chi_1^0}, \sigma_p^{\text{SI}})$ plane, however; the CMSSM’s prediction for σ_p^{SI} contains a factor of 10 uncertainty [42], which we incorporate with a method identical to that in e.g., Ref. [30].

Because we are, *a priori*, ignorant of the supersymmetry breaking scale, our priors for the soft parameters are invariant under rescalings, *i.e.*, we pick logarithmic priors for the soft masses m_0 and $m_{1/2}$,

$$\pi(x) \propto 1/x. \tag{11}$$

Table 2 Priors for the CMSSM model parameters

Parameter	Distribution
m_0	Log, 0.3–20 TeV
$m_{1/2}$	Log, 0.3–10 TeV
A_0	Flat, $ A_0 < 5m_0$
$\tan \beta$	Flat, 3–60
$\text{sign } \mu$	± 1 , with equal probability
$m_b(m_b)^{\overline{\text{MS}}}$	Gaussian, 4.18 ± 0.03 GeV [46]
m_t^{Pole}	Gaussian, 173.07 ± 0.89 GeV [46]
$1/\alpha_{\text{em}}(M_Z)^{\overline{\text{MS}}}$	Gaussian, 127.944 ± 0.014 [46]
$\alpha_s(M_Z)^{\overline{\text{MS}}}$	Gaussian, 0.1185 ± 0.0005 [46]

We will, however, investigate linear priors by re-weighting our posterior. We pick linear priors for the remaining parameters A_0 and $\tan \beta$. The principal motivation for supersymmetry is that it solves the “fine-tuning” problem that afflicts the SM [56], if the soft-breaking masses are sufficiently light [57,58]. For this reason, we restrict soft-breaking masses in our priors to less than 20 TeV, in accordance with what one might have believed prior to seeing experimental data from e.g., the LHC. Furthermore, Ref. [21] indicates that this choice omits no credible parts of the parameter space. We include the SM nuisance parameters $(m_t, m_b, \alpha_s$ and $1/\alpha_{\text{em}})$ with informative Gaussian priors, with their experimental means and variances from the Particle Data Group (PDG) [46]. Our priors are listed in Table 2. Furthermore, because our prior ranges and constraints are similar to those in Ref. [59], in which a simple “hard-cut” scanning algorithm was applied to the CMSSM, we can make a fair comparison between a Bayesian analysis and a simple method.

We plot the credible regions of the marginalized posterior on the $(m_0, m_{1/2})$ plane in Fig. 1a. One can identify by eye three modes on the $(m_0, m_{1/2})$ plane, which are characterized by the mechanism by which dark matter is annihili-

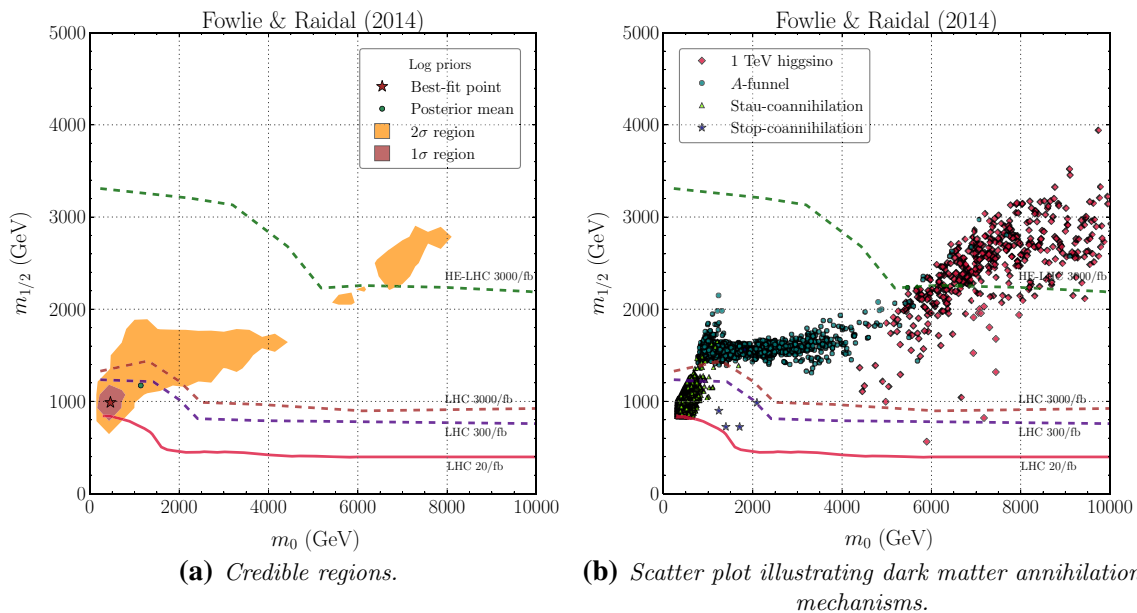


Fig. 1 The $(m_0, m_{1/2})$ plane of the CMSSM showing: (a) The 68 % (red) and 95 % (orange) credible regions of the marginalized posterior and (b) A scatter of the points with appreciable posterior weight colored

by their dominant dark matter annihilation mechanism. The expected discovery potentials of future hadron colliders are also shown

lated in the early Universe. The three dominant mechanisms present are:

- Stau-coannihilation with a bino-like neutralino at 1σ at light soft-breaking masses; $m_0 \sim 1$ TeV and $m_{1/2} \sim 1$ TeV. Because $m_{\chi_1^0} \simeq m_{\tilde{\tau}}$, stau-coannihilation is significant and proceeds via stau–tau–bino gauge interaction vertices in s - and t -channel diagrams. Such diagrams are suppressed if neutralinos are heavy, by a heavy t -channel stau or an off-shell s -channel tau.
- A-funnel s -channel annihilation at 2σ at intermediate soft-breaking masses; 0.5 TeV $\lesssim m_0 \lesssim 2$ TeV and $m_{1/2} \sim 1.5$ TeV. Because $m_{\chi_1^0} \simeq m_A/2$, neutralinos annihilate via an s -channel pseudo-scalar Higgs (which avoids helicity suppression, because the vertex is a Yukawa, and p -wave suppression, because it couples via the $L = 0$ partial wave). Annihilation is via a Higgs–higgsino–gaugino vertex; the neutralino must have a mixed composition, though it is dominantly bino-like. Satisfying $m_{\chi_1^0} \simeq m_A/2$ becomes impossible with heavy soft-breaking masses in the CMSSM, though is possible in MSSM models, in which m_A is a free parameter [60]. Note that with lighter m_A , supersymmetric contributions to $\text{BR}(B_s \rightarrow \mu\mu)$ are appreciable.
- The so-called “1 TeV higgsino region” [21,60,61] at 2σ at heavy soft-breaking masses; 5 TeV $\lesssim m_0 \lesssim 9$ TeV and 2 TeV $\lesssim m_{1/2} \lesssim 3$ TeV. The higgsino-like neutralino annihilates via a t -channel charged higgsino to WW with

higgsino–charged higgsino–gauge boson vertices or coannihilates with a higgsino-like chargino to an ff' pair. This region is similar in this regard to the focus-point. With heavier $\mu \gtrsim 1$ TeV, the relic density is increased. Because $\mu \gg M_W$, the mass splitting between the higgsino-like chargino and higgsino-like neutralinos is negligible. The higgsino-like chargino is “parasitic” in the language of Ref. [62] and increases the relic density. With lighter $\mu \lesssim 1$ TeV, the Higgs mass is lighter than its measured value. Because the neutralino is higgsino-like, the spin-independent scattering cross section with a proton, σ_p^{SI} , is enhanced via an s -channel Higgs diagram, with higgsino–bino–Higgs vertices. Although with $\mu < 0$, light and heavy Higgs bosons could destructively interfere, the heavy Higgs is so heavy that significant cancelations rarely occur. This region is disfavored by LUX, which at $m_{\chi_1^0} \simeq 1$ TeV restricts $\sigma_p^{\text{SI}} \lesssim 10^{-44}$ cm².

These mechanisms are not disjoint; A-funnel annihilation is present, though somewhat off-resonance, at heavier $m_{1/2}$ above the “1 TeV higgsino region.” A line of fine-tuned solutions exist from the A-funnel mode along the top of the “1 TeV higgsino region.” Although $m_{\chi_1^0} - m_A/2$ is increasing along this line, so too is the pseudoscalar’s width. Regardless of the dark matter annihilation mechanism and regardless of our priors, we find that the neutralino mass must be less than 1160 GeV at 95 % (one tail). In Fig. 2a, we see that the sizes of

the A -funnel and “1 TeV higgsino region” on the $(m_0, m_{1/2})$ plane are considerably increased if one uses linear priors, rather than logarithmic priors, and both are present at 1σ rather than 2σ .

Other mechanisms, *e.g.*, Z/h resonances and bulk annihilation, which could annihilate dark matter at a sufficient rate, are excluded by LHC direct searches for sparticles. Our posterior is, by eye, in good agreement with that in Ref. [21], which omits direct detection experiments, with $\Delta\chi^2$ plots in Ref. [19] and with crude results in Ref. [59]. Reference [21] identifies a “focus-point” region at $m_0 \sim 4$ TeV and $m_{1/2} \sim 1$ TeV. While we see a few such points in Fig. 1b at the beginning of the “1 TeV higgsino region,” their combined posterior weight is negligible, and they are absent in Fig. 1a. The “focus-point” struggles to produce $m_h \sim 125$ GeV and is disfavored by the LUX experiment. It might have an appreciable posterior weight in Ref. [21] because that analysis included a 3 GeV theory error (rather than our 2 GeV theory error) in the m_h calculation and omitted direct detection experiments.

Reference [59] identified stop coannihilation as a possible dark matter annihilation mechanism. Because the MultiNest-2.18 algorithm found few such solutions (although we confirm that such points with reasonable χ^2 exist), the stop-coannihilation regions are fine-tuned so much so that their posterior weight is negligible. We plot stop-coannihilation solutions in Fig. 1b.

On the $(A_0, \tan\beta)$ plane in Fig. 3, we identify two modes that correspond to the stau-coannihilation and A -funnel regions on the $(m_0, m_{1/2})$ plane. The stau-coannihilation region prefers $\tan\beta \lesssim 30$ and negative A_0 to achieve the required mass degeneracy and stop mixing. Within the stau-coannihilation region, $\mu > 0$ is preferred to enhance δa_μ with light sparticle loops. The A -funnel requires $\tan\beta \simeq 50$ and prefers $A_0 \gtrsim 1.5$ TeV so that the pseudo-scalar Higgs is sufficiently light.

Our posterior on this plane is, by eye, in agreement with $\Delta\chi^2$ plots in Ref. [19], but in poor agreement with that in Ref. [21]. In each case, one can identify a stau-coannihilation region at small $\tan\beta$. We, however, fail to see modes at $A_0 \sim \pm 8$ TeV present in Ref. [21], corresponding to the “1 TeV higgsino region.” The higgsino-like neutralino is disfavored by the LUX direct search for dark matter. No direct detection constraint was applied in Ref. [21], though its potential impact was investigated and found to be substantial in the “1 TeV higgsino region,” in agreement with our findings. That the “1 TeV higgsino region” is present on the $(m_0, m_{1/2})$ plane but not on the $(A_0, \tan\beta)$ plane is a result of marginalization. Acceptable $\mu \simeq 1$ TeV solutions result from a moderate range of $(A_0, \tan\beta)$, but a rather restricted range of $(m_0, m_{1/2})$. On the $(m_0, m_{1/2})$ plane in the “1 TeV higgsino region,” the posterior weight is enhanced by the many $(A_0, \tan\beta)$ solutions, whereas, on the $(A_0, \tan\beta)$

plane in the “1 TeV higgsino region,” the posterior weight is the sum of few $(m_0, m_{1/2})$ solutions.

The “1 TeV higgsino region” is, however, visible on the $(A_0, \tan\beta)$ plane with linear priors in Fig. 2b with $\tan\beta \sim 45$ and $10 \text{ TeV} \lesssim A_0 \lesssim 20 \text{ TeV}$. Large A_0 and $\tan\beta$ are preferred to achieve $\mu \sim 1$ TeV and to ensure that radiative electroweak symmetry breaking with $m_{H_u}^2 < 0$ is achieved, in spite of such heavy m_0 . Because the stop-coannihilation mechanism requires large a_t at the electroweak scale to split the stops so that the lightest is degenerate with the neutralino, it prefers large negative A_0 .

On the $(m_{\chi_1^0}, \sigma_p^{SI})$ plane in Fig. 4, which is relevant to direct searches for dark matter, we again identify three modes characterized by their dark matter annihilation mechanism: the stau-coannihilation region at $m_{\chi_1^0} \sim 500$ GeV, the A -funnel at $m_{\chi_1^0} \sim 700$ GeV and the “1 TeV higgsino region.” As anticipated, the scattering cross section is largest in the “1 TeV higgsino region,” because the higgsino–bino–Higgs vertices are enhanced by the neutralino’s composition. Linear priors (Fig. 4b) favor the “1 TeV higgsino region.” The LUX limit was, of course, included in our likelihood function; *prima facie* it is surprising that the “1 TeV higgsino region” lies above that limit. This is because there is significant theoretical uncertainty in the scattering cross sections. There is an appreciable chance that regions with *calculated* scattering cross sections that are above the LUX limit in fact have *true* scattering cross sections that are below the LUX limit. Our Bayesian methodology and results reflect this fact.

To conclude, let us summarize the impact of the experimental measurements in our likelihood function in Table 1:

- If the relic density, Ωh^2 , is to be sufficiently small, the neutralino’s mass or composition must be fine-tuned to enhance a particular annihilation mechanism. This selects narrow regions of parameter space.
- The Higgs mass, $m_h \sim 125$ GeV, prefers intermediate soft-breaking masses or $\lesssim 1$ TeV soft-breaking masses and maximal stop mixing. Higgsino-like neutralinos with either $m_0 \lesssim 5$ TeV or $m_0 \gtrsim 10$ TeV are disfavored. The W -boson mass, M_W , further disfavors $m_h \gtrsim 125$ GeV, even if sparticle-loop contributions are negligible [63].
- The null result of the LUX direct search for dark matter disfavors higgsino-like neutralinos.
- The effect of LHC direct searches is somewhat trivial; a low-mass portion of the $(m_0, m_{1/2})$ plane is excluded.
- With heavy sparticles, sparticle-loop contributions to electroweak precision observables and b -physics are insubstantial, and their impact is somewhat limited. A positive sign of the Higgs parameter is favored by δa_μ in the stau-coannihilation region, in which sparticles are light. Furthermore, $\text{BR}(B_s \rightarrow \mu\mu)$ disfavors light pseudo-scalar Higgs masses, which could enhance $\text{BR}(B_s \rightarrow \mu\mu)$,

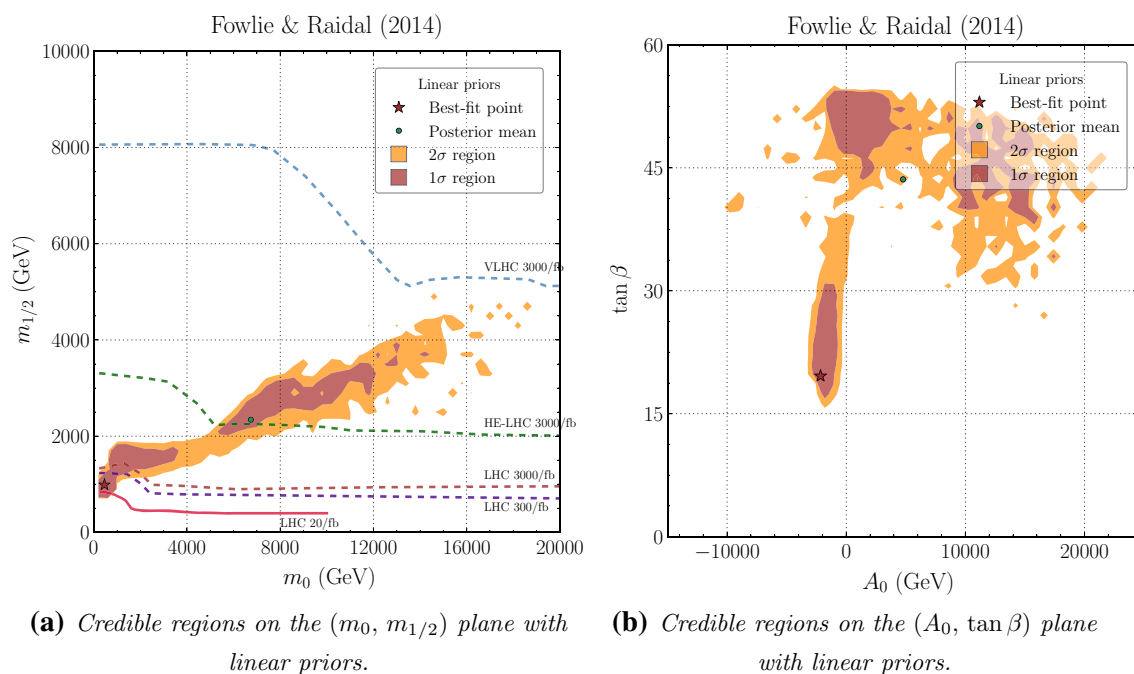


Fig. 2 The $(m_0, m_{1/2})$ and $(A_0, \tan \beta)$ planes of the CMSSM showing the 68 % (red) and 95 % (orange) credible regions of the marginalized posterior. The expected discovery potentials of future hadron colliders are also shown

which in turn disfavors A -funnel annihilation if the neutralino is light.

4 Results and discussion

For concreteness, we say that a CMSSM point is discoverable if, were nature described by that CMSSM point, it is expected that the SM background hypothesis could be rejected at 5σ . We assume that two simplified channels [64] studied in Ref. [65] describe the hadron collider phenomenology of the CMSSM’s favored regions:

- If gluinos and squarks are light, we assume a simplified gluino–squark–neutralino channel in which gluinos and squarks are pair produced and decay to a neutralino and a quark or quark pair. Because the neutralinos must be less than approximately 1 TeV at 95 % from our posterior, one can expect a discovery potential of $m_{\tilde{g}} \simeq m_{\tilde{q}} \lesssim 2.7$ TeV ($m_{\tilde{g}} \simeq m_{\tilde{q}} \lesssim 3.0$ TeV) at the LHC with 300/fb (3000/fb), $m_{\tilde{g}} \simeq m_{\tilde{q}} \lesssim 6.6$ TeV at the HE-LHC, and $m_{\tilde{g}} \simeq m_{\tilde{q}} \lesssim 15$ TeV at the VLHC with 3000/fb [65].
- If squarks are heavy, we assume a simplified gluino–neutralino channel in which gluinos are pair produced and decay to a neutralino and a quark pair via an off-shell squark. Because the neutralinos must be less than approximately 1 TeV at 95 % from our posterior, one can expect a discovery potential of $m_{\tilde{g}} \lesssim 1.9$ TeV ($m_{\tilde{g}} \lesssim 2.2$ TeV)

at the LHC with 300/fb (3000/fb), $m_{\tilde{g}} \lesssim 5.0$ TeV at the HE-LHC, and $m_{\tilde{g}} \lesssim 11$ TeV at the VLHC with 3000/fb [65].

We neglect electroweak production, which is unlikely to significantly extend the discovery potential at a hadron collider.

The discovery potential of the various experiments is shown on the $(m_0, m_{1/2})$ planes in Figs. 1 and 2 for logarithmic and linear priors, respectively. For logarithmic priors, the LHC with 300/fb could discover all of the CMSSM’s stau-coannihilation region and a light fraction of the A -funnel region while the HE-LHC could discover all of the A -funnel. The “1 TeV higgsino region,” however, is entirely beyond the reach of the LHC, and partially beyond that of the HE-LHC. For linear priors, large part of the A -funnel region remains uncovered also by the HE-LHC. However, for the VLHC our conclusion is the same for both choices of the prior: the CMSSM can be discovered for all favored dark matter annihilation mechanisms. We stress once more the complementarity between collider searches and direct detection, as seen in Fig. 4. Improving direct detection constraints and/or reducing the associated nuclear uncertainties could entirely exclude the “1 TeV higgsino region.”

It is evident that our results, which we calculate from Eq. (8), are somewhat sensitive to our choice of priors. We calculated our probabilities with linear priors and logarithmic priors for the soft-breaking masses. Linear priors weight linear intervals evenly, *i.e.*, $\pi(x) \propto \text{constant}$. While different

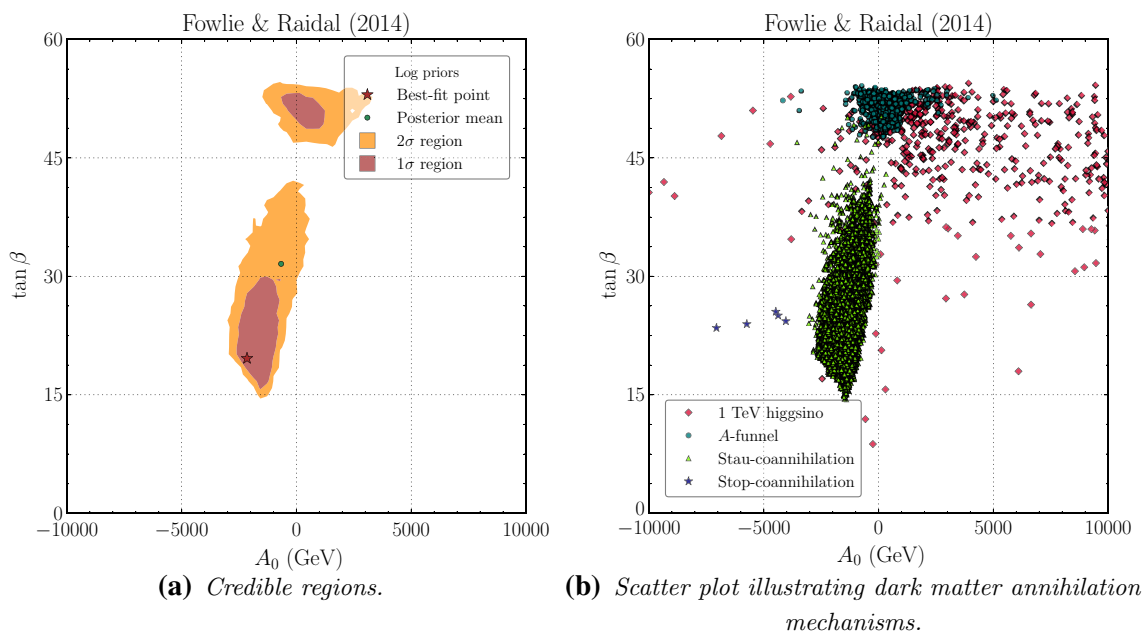


Fig. 3 The $(m_0, m_{1/2})$ plane of the CMSSM showing: (a) The 68 % (red) and 95 % (orange) credible regions of the marginalized posterior and (b) a scatter of the points with appreciable posterior weight colored by their dominant dark matter annihilation mechanism

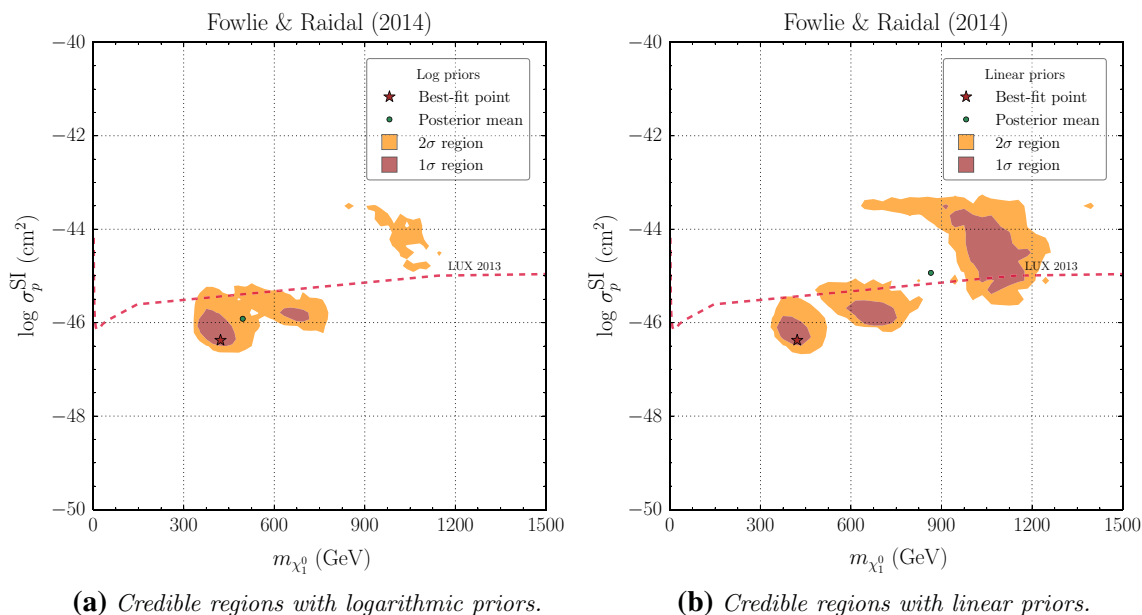


Fig. 4 The 68 % (red) and 95 % (orange) credible regions of the marginalized posterior on the $(m_{\chi_1^0}, \sigma_p^{SI})$ plane. The 90 % exclusion contour from LUX is also shown

investigators might have a spectrum of prior beliefs for the CMSSM’s parameters, all investigators ought to make identical conclusions from their posteriors, if the experimental data is “strong enough.” Although we believe that, because they are scale invariant, logarithmic priors for the soft-breaking masses are the best choice, linear priors are not unreasonable. We checked that a $\pm 10\%$ systematic uncertainty in the expected hadron collider discovery reach had limited impact

compared to that of our prior choice. In the paragraphs that follow, we quote the range of probabilities obtained from logarithmic and linear priors rounded to the nearest whole 5 %. Note that null results from future direct detection and $BR(B_s \rightarrow \mu\mu)$ experiments would disfavor the A-funnel and “1 TeV higgsino region.” Because those regions are disfavored by logarithmic priors, if in the future such experiments were to obtain null results, the probabilities calculated

Table 3 Probability of discovering SUSY at various experiments with logarithmic and linear priors. All probabilities are conditioned on experimental data thus far obtained and on the assumption that the CMSSM

Experiment	Probability of discovering SUSY, given data, CMSSM correct model		...and given that previous experiment did not discover the CMSSM	
	Log priors	Linear priors	Log priors	Linear priors
LHC 300/fb	73 %	15 %	–	–
LHC 3000/fb	76 %	17 %	9 %	2 %
HE-LHC 3000/fb	96 %	45 %	83 %	34 %
VLHC 3000/fb	100 %	100 %	100 %	100 %

is the correct model. In the second set of two columns, the probability is also conditioned on the proposition that the previous collider experiments in the table failed to discover SUSY

with logarithmic priors would be more accurate than those with linear priors.

We find that from Eq. (8), the probability that the CMSSM could be discovered at the VLHC is always 100 %, at the HE-LHC, 45–95 % and at the LHC with 300/fb (3000/fb), 15–75 % (15–75 %). All probabilities are conditional on the experimental data obtained thus far and on the assumption that the CMSSM is the true model.

It is instructive, however, to consider the probability of a discovery at a hypothetical experiment given that all experiments including hypothetical experiments that would have been performed by that time did not make a discovery, e.g.,

$$\begin{aligned}
 & p(\text{Discoverable at HE-LHC} \mid \text{data, model, No LHC experiments make a discovery}) \\
 &= \frac{p(\text{Discoverable at HE-LHC, Not discoverable at LHC} \mid \text{data, model})}{p(\text{Not discoverable at LHC} \mid \text{data, model})} \\
 &= \frac{p(\text{Discoverable at HE-LHC} \mid \text{data, model}) - p(\text{Discoverable at LHC} \mid \text{data, model})}{1 - p(\text{Discoverable at LHC} \mid \text{data, model})}.
 \end{aligned}
 \tag{12}$$

With this caveat the probability of discovering the CMSSM at the LHC with 3000/fb is 1–10 % and at the HE-LHC, 35–85 %. Our probabilities suggest that the HE-LHC is rather likely to discover SUSY, assuming that the CMSSM is the correct model. The VLHC should have the final word on the CMSSM; we find with near certainty that if the CMSSM is the correct model, the VLHC will discover SUSY. The LHC 3000/fb is unlikely to discover the CMSSM, if it was not already discovered with 300/fb. We summarize all probabilities in Table 3.

Our probabilities were, of course, dependent on our assumption that the dark matter is entirely neutralino. We recalculated the probabilities with the minimal assumption that the CMSSM accounted for only the Higgs boson mass, by including only the measurement of the Higgs mass in our likelihood function. We permitted, *a priori*, $\tan \beta \simeq 1$, which is disfavored by e.g., the dark matter relic density measurement, but which reduces the tree-level Higgs mass. In all our results, however, we vetoed points for which Yukawa cou-

plings were non-perturbative below the GUT scale or points that were otherwise unphysical.

The resulting posterior is plotted in Fig. 5 for the $(m_0, m_{1/2})$ and for stop–gluino mass planes.¹ The effect of giving up the requirement of obtaining the observed amount of DM is evident: part of the high mass parameter region remains uncovered by all the planned colliders. While the credible regions suggest that the VLHC has an appreciable (85 %) probability of discovering the CMSSM, this conclusion is somewhat dependent on our priors. Soft-breaking masses of greater than ~ 10 TeV typically result in a Higgs mass that is greater than its measured value, but are also

disfavored by our logarithmic priors. With linear priors for m_0 and $m_{1/2}$, that probability is moderate (50 %). The results plotted in Fig. 5 demonstrate that DM annihilation processes do constrain the SUSY parameters significantly.

We assumed that $m_{1/2} \leq 10$ TeV and $m_0 \leq 20$ TeV in our priors in Table 2; this choice omitted no credible parts of parameter space or DM annihilation mechanisms. To check whether our probabilities were sensitive to this assumption, we reduced our prior ranges to $m_{1/2} \leq 5$ TeV and $m_0 \leq 10$ TeV and recalculated our probabilities. With logarithmic priors, the probabilities changed by ~ 1 percentage point, because the 95 % credible region on the $(m_0, m_{1/2})$ plane in Fig. 1 was within $m_{1/2} \leq 5$ TeV and $m_0 \leq 10$ TeV. With linear priors, the 95 % credible region on the $(m_0, m_{1/2})$ plane in Fig. 2 exceeded $m_0 \leq 10$ TeV in the “1 TeV higgsino region;” applying the prior range $m_0 \leq 10$ TeV truncated the “1 TeV higgsino region.” The probabilities for the LHC

¹ A similar result was first found in Ref. [21].

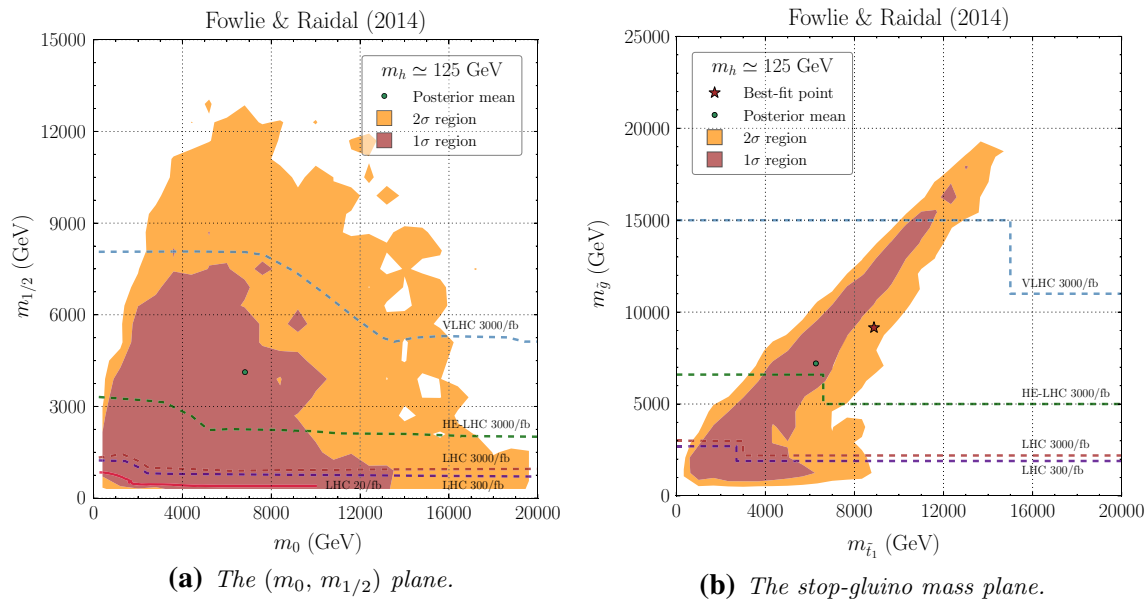


Fig. 5 The CMSSM 68 % (red) and 95 % (orange) credible regions of the marginalized posterior with only the measurement of the Higgs mass in our likelihood function and with logarithmic priors. The expected discovery potentials of future hadron colliders are also shown

increased by ~ 5 percentage points, whereas that for the HE-LHC decreased by ~ 20 percentage points. The probability for the VLHC was unchanged. This indicates sensitivity to the prior range for m_0 . We believe, however, that our prior range for m_0 was a fair choice, because, unlike the reduced prior range, our choice omitted no viable DM annihilation mechanisms.

5 Conclusions

While in the near future experiments at the LHC are expected to continue at $\sqrt{s} = 14$ TeV, discussions are under way for a high-energy proton–proton collider. Two preliminary ideas are the $\sqrt{s} = 100$ TeV VLHC and the $\sqrt{s} = 33$ TeV HE-LHC. We calculated the Bayesian posterior density of the CMSSM’s parameter space, given experimental data from the LHC, LUX, and Planck. Our result was in agreement with similar previous analyses and could be understood with reference to possible dark matter annihilation mechanisms. With Bayesian statistics, we calculated the probabilities that the LHC, HE-LHC, and VLHC discover SUSY in the future, assuming that nature is described by the CMSSM and given the experimental data from the LHC, LUX, and Planck (*e.g.*, assuming that dark matter is entirely neutralino).

We found that the LHC with 300/fb at $\sqrt{s} = 14$ TeV has a 15–75 % probability of discovering SUSY. If that experiment does not discover SUSY, the probability of discovering SUSY with 3000/fb is merely 1–10 %. Were SUSY to remain undetected at the LHC, the HE-LHC would have a 35–85 % probability of discovering SUSY with 3000/fb. The VLHC, on the other hand, ought to be definitive; it has

a 100 % probability of discovering SUSY with 3000/fb. All probabilities, summarized in Table 3, are conditional on the experimental data obtained thus far and on the assumption that the CMSSM is the true model. We remind the reader that in Bayesian statistics, probability is a numerical measure of belief, and it is sensitive to one’s prior beliefs, *e.g.*, our priors for the CMSSM in Table 2, though we believe our priors were fair. Nevertheless, our finding that the VLHC has a 100 % probability of discovering SUSY with 3000/fb was independent of our choice of prior for the soft-breaking masses. We checked that our conclusions were robust with respect to systematic errors in the expected performance of the collider experiments.

Stated qualitatively, our conclusions are that there is a fair probability of discovering the CMSSM at the LHC with 300/fb at $\sqrt{s} = 14$ TeV. If that search is unsuccessful, the CMSSM is unlikely to be discovered in 3000/fb. A $\sqrt{s} = 33$ TeV HE-LHC with 3000/fb would be likely to discover the CMSSM, and, should it be unsuccessful, a $\sqrt{s} = 100$ TeV VLHC would definitively discover the CMSSM.

Our results were primarily determined by the CMSSM’s predictions for the Higgs mass and the DM abundance, which we assumed to be entirely neutralinos. If, however, DM has a different origin, the CMSSM could be unreachable even at the VLHC. Our conclusions are applicable to only the CMSSM; in relaxed models, one can tune the pseudo-scalar resonance so that heavy neutralinos are annihilated at a sufficient rate.

Acknowledgments We thank M. Kadastik for helpful discussions. This work was supported in part by grants IUT23-6, CERN+, and by the European Union through the European Regional Development Fund and by ERDF project 3.2.0304.11-0313 Estonian Scientific Computing Infrastructure (ETAIS).

Open Access This article is distributed under the terms of the Creative Commons Attribution License which permits any use, distribution, and reproduction in any medium, provided the original author(s) and the source are credited.

Funded by SCOAP³ / License Version CC BY 4.0.

References

1. A. Salam, J. Strathdee, Nucl. Phys. **B76**, 477 (1974)
2. H.E. Haber, G.L. Kane, Phys. Rept. **117**, 75 (1985)
3. H.P. Nilles, Phys. Rept. **110**, 1 (1984)
4. H. Georgi, S. Glashow, Phys. Rev. Lett. **32**, 438 (1974)
5. S. Dimopoulos, H. Georgi, Nucl. Phys. **B193**, 150 (1981)
6. G. Jungman, M. Kamionkowski, K. Griest, Phys. Rept. **267**, 195 (1996). [arXiv:hep-ph/9506380](#)
7. R. Assmann, R. Bailey, O. Brning, O. Dominguez Sanchez, G. de Rijk, J. M. Jimenez, S. Myers, L. Rossi, L. Taviani, E. Todesco, et al., Tech. Rep. CERN-ATS-2010-177, CERN, Geneva (2010)
8. Future Circular Collider Kickoff Meeting (University of Geneva, Geneva, Switzerland, 2014). <http://indico.cern.ch/conferenceDisplay.py?confId=282344>
9. T.J. LeCompte, S.P. Martin, Phys. Rev. **D84**, 015004 (2011). [arXiv:1105.4304](#)
10. P. Fayet, Nucl. Phys. **B90**, 104 (1975)
11. U. Ellwanger, C. Hugonie, A.M. Teixeira, Phys. Rept. **496**, 1 (2010). [arXiv:0910.1785](#)
12. R. Trotta, Contemp. Phys. **49**, 71 (2008). [arXiv:0803.4089](#)
13. A.H. Chamseddine, R.L. Arnowitt, P. Nath, Phys. Rev. Lett. **49**, 970 (1982)
14. R.L. Arnowitt, P. Nath, Phys. Rev. Lett. **69**, 725 (1992)
15. G.L. Kane, C.F. Kolda, L. Roszkowski, J.D. Wells, Phys. Rev. **D49**, 6173 (1994). [arXiv:hep-ph/9312272](#)
16. C. Beskidt, W. de Boer, D. Kazakov (2014). [arXiv:1402.4650](#)
17. T. Cohen, J.G. Wacker, JHEP **1309**, 061 (2013). [arXiv:1305.2914](#)
18. S. Henrot-Versill, R. Lafaye, T. Plehn, M. Rauch, D. Zerwas, et al. (2013). [arXiv:1309.6958](#)
19. O. Buchmueller, R. Cavanaugh, A. De Roeck, M. Dolan, J. Ellis, et al. (2013). [arXiv:1312.5250](#)
20. P. Bechtle, K. Desch, H. K. Dreiner, M. Hamer, M. Krmer, et al. (2013). [arXiv:1310.3045](#)
21. K. Kowalska, L. Roszkowski, E.M. Sessolo, JHEP **1306**, 078 (2013). [arXiv:1302.5956](#)
22. A. Fowlie, M. Kazana, K. Kowalska, S. Munir, L. Roszkowski et al., Phys. Rev. **D86**, 075010 (2012). [arXiv:1206.0264](#)
23. L. Roszkowski, E.M. Sessolo, Y.-L.S. Tsai, Phys. Rev. **D86**, 095005 (2012). [arXiv:1202.1503](#)
24. C. Streye, G. Bertone, F. Feroz, M. Fornasa, R. R. de Austri, et al. (2012). [arXiv:1212.2636](#)
25. B. Allanach, T. Khoo, C. Lester, S. Williams, JHEP **1106**, 035 (2011). [arXiv:1103.0969](#)
26. S. Akula, P. Nath, G. Peim, Phys. Lett. **B717**, 188 (2012). [arXiv:1207.1839](#)
27. M. E. Cabrera, J. A. Casas, R. R. de Austri (2012). [arXiv:1212.4821](#)
28. F. Feroz, M. Hobson, M. Bridges, Mon. Not. Roy. Astron. Soc. **398**, 1601 (2009). [arXiv:0809.3437](#)
29. J. Buchner, A. Georgakakis, K. Nandra, L. Hsu, C. Rangel, et al. (2014). [arXiv:1402.0004](#)
30. A. Fowlie, A. Kalinowski, M. Kazana, L. Roszkowski, Y.-L.S. Tsai, Phys. Rev. **D85**, 075012 (2012). [arXiv:1111.6098](#)
31. G. Belanger, F. Boudjema, P. Brun, A. Pukhov, S. Rosier-Lees et al., Comput. Phys. Commun. **182**, 842 (2011). [arXiv:1004.1092](#)
32. G. Belanger, F. Boudjema, A. Pukhov, A. Semenov, Comput. Phys. Commun. **176**, 367 (2007). [arXiv:hep-ph/0607059](#)
33. S. Heinemeyer, W. Hollik, G. Weiglein, Comput. Phys. Commun. **124**, 76 (2000). [arXiv:hep-ph/9812320](#)
34. S. Heinemeyer, W. Hollik, G. Weiglein, Eur. Phys. J. **C9**, 343 (1999). [arXiv:hep-ph/9812472](#)
35. G. Degrossi, S. Heinemeyer, W. Hollik, P. Slavich, G. Weiglein, Eur. Phys. J. **C28**, 133 (2003). [arXiv:hep-ph/0212020](#)
36. M. Frank, T. Hahn, S. Heinemeyer, W. Hollik, H. Rzehak et al., JHEP **0702**, 047 (2007). [arXiv:hep-ph/0611326](#)
37. B. Allanach, Comput. Phys. Commun. **143**, 305 (2002). [arXiv:hep-ph/0104145](#)
38. The ATLAS collaboration. Search for squarks and gluinos with the ATLAS detector in final states with jets and missing transverse momentum and 20.3 fb^{-1} of $\sqrt{s} = 8 \text{ TeV}$ proton-proton collision data. Tech. Rep. ATLAS-CONF-2013-047, ATLAS-COM-CONF-2013-049 (2013)
39. B. Allanach, Phys. Rev. **D83**, 095019 (2011). [arXiv:1102.3149](#)
40. P. Bechtle, B. Sarrazin, K. Desch, H.K. Dreiner, P. Wienemann et al., Phys. Rev. **D84**, 011701 (2011). [arXiv:1102.4693](#)
41. D. Akerib et al. (LUX Collaboration) (2013). [arXiv:1310.8214](#)
42. J.R. Ellis, K.A. Olive, C. Savage, Phys. Rev. **D77**, 065026 (2008). [arXiv:0801.3656](#)
43. P. Ade et al. (Planck Collaboration) (2013). [arXiv:1303.5076](#)
44. B. C. Allanach, G. Belanger, F. Boudjema, A. Pukhov, pp. 961–964 (2004). [arXiv:hep-ph/0410049](#)
45. B. Allanach, G. Belanger, F. Boudjema, A. Pukhov, W. Porod (2004). [arXiv:hep-ph/0402161](#)
46. J. Beringer et al., Particle Data Group. Phys. Rev. **D86**, 010001 (2012)
47. S. Chatrchyan et al. (CMS Collaboration), Phys. Lett. **B716**, 30 (2012). [arXiv:1207.7235](#)
48. G. Aad et al. (ATLAS Collaboration), Phys. Lett. **B716**, 1 (2012). [arXiv:1207.7214](#)
49. B. Allanach, A. Djouadi, J. Kneur, W. Porod, P. Slavich, JHEP **0409**, 044 (2004). [arXiv:hep-ph/0406166](#)
50. S. Heinemeyer, W. Hollik, G. Weiglein, Phys. Rept. **425**, 265 (2006). [arXiv:hep-ph/0412214](#)
51. R. Trotta, F. Feroz, M.P. Hobson, L. Roszkowski, R. Ruiz de Austri, JHEP **0812**, 024 (2008). [arXiv:0809.3792](#)
52. R.R. de Austri, R. Trotta, L. Roszkowski, JHEP **0605**, 002 (2006). [arXiv:hep-ph/0602028](#)
53. Y. Amhis et al. (Heavy Flavor Averaging Group) (2012). [arXiv:1207.1158](#)
54. M. Misiak, H. Asatrian, K. Bieri, M. Czakon, A. Czarnecki et al., Phys. Rev. Lett. **98**, 022002 (2007). [arXiv:hep-ph/0609232](#)
55. O. Buchmueller, R. Cavanaugh, A. De Roeck, M. Dolan, J. Ellis et al., Eur. Phys. J. **C72**, 1878 (2012). [arXiv:1110.3568](#)
56. L. Susskind, Phys. Rev. **D20**, 2619 (1979)
57. R. Barbieri, G. Giudice, Nucl. Phys. **B306**, 63 (1988)
58. J.R. Ellis, K. Enqvist, D.V. Nanopoulos, F. Zwirner, Mod. Phys. Lett. **A1**, 57 (1986)
59. M. Kadastik, K. Kannike, A. Racioppi, M. Raidal, JHEP **1205**, 061 (2012). [arXiv:1112.3647](#)
60. A. Fowlie, K. Kowalska, L. Roszkowski, E.M. Sessolo, Y.-L.S. Tsai, Phys. Rev. **D88**, 055012 (2013). [arXiv:1306.1567](#)
61. L. Roszkowski, R. Ruiz de Austri, R. Trotta, Y.-L.S. Tsai, T.A. Varley, Phys. Rev. **D83**, 015014 (2011). [arXiv:0903.1279](#)
62. S. Profumo (2013). [arXiv:1301.0952](#)
63. S. Heinemeyer, W. Hollik, G. Weiglein, L. Zeune, JHEP **1312**, 084 (2013). [arXiv:1311.1663](#)
64. D. Alves et al. (LHC New Physics Working Group), J. Phys. **G39**, 105005 (2012). [arXiv:1105.2838](#)
65. T. Cohen, T. Golling, M. Hance, A. Henrichs, K. Howe, et al. (2013). [arXiv:1311.6480](#)